

Methods of gas hydrate concentration estimation with field examples

Dhananjay Kumar¹, Ranjan Dash¹, and Pawan Dewangan²

¹*Chevron Energy Technology Company, California, USA*

²*National Institute of Oceanography, Goa, India*

Abstract

The presence of gas hydrates alters the bulk physical properties of the host sediments. The deviation of the physical property in the hydrated layer from the regional (hydrate-free background) trend can be used to estimate hydrate concentration. In this paper, we summarize six different methods of gas hydrate concentration estimation that make use of data from the measurements of the seismic properties, electrical resistivity, chlorinity, porosity, density, and temperature. We demonstrate the methods of hydrate concentration estimation using data from three different geographical areas: 1) Mount Elbert test site, Alaska, 2) Cascadia margin, offshore Canada and 3) Krishna Godavari (KG) basin, offshore India. Based on our estimation, the hydrate saturation in the hydrate stability zone varies from 40% to 80% of pore space in Alaska, 10% to 40% of pore space in the Cascadia margin, and 5% to 40% of pore space in the KG basin. There are various factors that can affect the hydrate saturation estimate; the two most important factors being the background property value in the absence of gas hydrate, and the modeling relationship between the physical property and gas hydrate saturation. We also present a simple work-flow for hydrate saturation estimation from seismic velocity in a Microsoft Excel sheet.

Introduction

Gas hydrate is a solid, ice-like, crystalline substance containing low molecular weight gases (mostly methane) in a lattice of water molecules (Sloan, 1998). The formation and stability of gas hydrates within the subsurface depend upon the supply of free gas in excess of the solubility limit, suitable pressure and temperature conditions, pore fluid chemistry and the nature of the trapped gas. Globally, hydrates are found in ocean floor sediments at water depths greater than about 500 m and in permafrost environments.

Hydrates contain an immense amount of natural gas (Collett, 2002) and have the potential to be a future clean energy resource. Although estimations vary widely as there is no standard method for estimating hydrate concentration, the amount of free gas within oceanic hydrates can be as high as $21 \times 10^{15} \text{ m}^3$ (Kvenvolden, 1999) or $1.5 \times 10^{15} \text{ m}^3$ (Milkov, 2004). There are various publications on the gas hydrate concentration estimation from different geological and geophysical measurements (e.g., Lee et al., 1996; Tinivella, 1999; Ecker et al., 2000; Lu and McMechan, 2002; Carcione and Gei, 2004; Kumar et al., 2007; Westbrook, 2008). In this article, we aim to summarize different methods available for estimating gas hydrate concentration and demonstrate those using well log data from three geographical areas: 1) BP-DOE-US "Mount Elbert" test, Alaska, 2) northern Cascadia margin offshore western Canada, and 3) Krishna Godavari (KG) basin, offshore India.

The presence of gas hydrates within the sediment pore space alters the mechanical properties of the host sediments (e.g., increasing the seismic velocities), and this change in properties from a background (hydrate free sediments) value can be utilized to estimate hydrate concentration. Finding a background value of physical properties is not trivial and it requires the knowledge of the

geological settings, use of analogs and other available data.

The hydrate concentration estimation procedure then requires formulating an appropriate relationship to describe the change in mechanical properties of the sediment with gas hydrate concentration. However, the accuracy of the estimation will depend on the sensitivity of these physical properties to the presence of gas hydrate e.g., higher the sensitivity of property more reliable is the estimation of hydrate concentration. Physical properties such as the seismic velocity and electrical resistivity are very sensitive to the presence of gas hydrate, while others like seismic anisotropy and attenuation are less sensitive. The relationship between a physical property and gas hydrate concentration may also depend on the nature of gas hydrates within the host sediment (filling of pore spaces, part of solid frame, fracture filling or as cement). In this paper, we assume hydrates as pore filling reducing the porosity of host sediments. There are various empirical and rock physics based relationships available between gas hydrate and physical properties (Lee et al., 1996; Helgerud et al., 1999; Chand et al., 2004; Kumar et al., 2007). However, many relationships are good for certain geological settings only and need field based selection of a modeling relationship. The following properties are commonly used to estimate the gas hydrate concentration:

1. Seismic or elastic properties (velocities, Poisson's ratio, impedance, AVA, anisotropy, attenuation)
2. Electrical resistivity
3. Chloride measurements of pore fluid
4. NMR-DENSITY porosity
5. Density
6. Temperature

In this paper we describe the methods of estimating gas-hydrate concentration using the properties listed above and demonstrate their applications with data from three

different geographic regions.

Methods

Before discussing various gas hydrate concentration estimation methods, we define two key terms used in this article: *saturation* and *concentration*. Hydrate saturation (S_h) is the volumetric fraction of hydrates present in the pore space, whereas hydrate concentration (S_{hyd}) is the volumetric fraction of hydrates in the sediment. Given the total porosity (ϕ) of the rock, saturation and concentration can be estimated from one another by the following relation:

$$S_{hyd} = \phi S_h \quad (1)$$

Seismic or elastic properties

Seismic reflection data have been historically used to remotely sense the presence of gas hydrates in marine sediments. The most common seismic proxy for gas hydrates is the BSR or the bottom simulating reflector, which represents the base of the gas hydrate stability zone (GHSZ) and mimics the seafloor. The BSR is caused by strong acoustic impedance contrast between the overlying hydrate bearing sediments and the underlying gas charged sediments. P-wave velocity (V_p) is commonly used to estimate gas hydrate concentration within the sediments (Singh et al., 1993; Ecker et al., 2000; Lu and McMechan, 2002). However, estimations based on V_p alone are not accurate enough when hydrates are present in low quantity (Lee et al., 1996; Yun et al., 2005). In such cases, V_p along with V_s (S-wave velocity) or V_p/V_s ratio (or Poisson's

ratio) may provide better constraints on the estimation (Kumar et al., 2007; Westbrook, 2008). In cases where free gas exists within the GHSZ (Lee and Collett, 2006; Kumar et al., 2007), V_s is required along with V_p to distinguish the effect of free gas and hydrate.

Seismic velocities (V_p and V_s) can be estimated from sonic logs (one dimensional data), seismic data (two and three dimensional data) and laboratory tests. For example, Waite et al. (2000) estimated a V_p of 3650 m/s, a V_s of 1890 m/s and a density of 900 kg/m³ from laboratory tests on pure synthetic hydrates. Although conventional seismic data can provide V_p easily, in most cases V_s has to be computed through indirect methods such as from the AVA (amplitude variation with angle) response of P-wave seismic data. However, where multicomponent data are available (for example from ocean bottom seismometers), V_s can be computed more accurately. Waveform inversion of seismic data (Korenga et al., 1997) can provide more reliable and higher resolution seismic velocity than conventional velocity analysis methods. If waveform seismic data are less reliable, amplitude data can be used for AVA inversion (Ojha and Sain, 2007) for impedance (equals velocity times density) and this impedance can be used to estimate gas hydrate concentration. Dai et al (2004) used impedance data to estimate hydrate concentration via a rock physics relationship based on effective medium modeling. Willoughby and Edwards (1997) used seafloor compliance data, which is sensitive to S-wave velocity change, to improve hydrate resource evaluation.

Several authors have presented relationships between seismic velocities and gas hydrate concentration

	A	B	C	D	E	F	G	H	I	J	K	L	DF
1	DEPTH (ft)	Measured Vp (m/s)	Porosity (fraction)	Background Vp (m/s)	Sh from Vp: method1	Sh from Vp: method2	Input values	Vpsho (Vp for Sh=0)	A table of seismic velocity (Vp) error (modeled Vp - measured Vp) for different gas hydrate saturations and given porosity values				
2	Well Logs			For hydrate-free sediment	Sh values are multiplied by 100		Vg (m/s)	Modeled background Vp	Sg	0.00	0.00	0.00	0.00
3							Sw	1.00	0.99	0.98	0.00		
4							Sh	0.00	0.01	0.02	1.00		
5							601.46	593.08	584.62	832.70			
6	2050.5	2601.5	0.37	2000	55	55.4	0.23	2848.96	Velocity error = modeled Vp (scaled by scalar1) - measured Vp	554.79	546.54	538.22	839.91
7	2051.0	2554.8	0.36	2000	53	52.9	Vw (m/s)	2900.65	530.24	522.00	513.70	859.44	
8	2051.5	2530.2	0.36	2000	51	51.1	1500	2907.31	516.17	507.88	499.52	889.12	
9	2052.0	2516.2	0.36	2000	50	49.7	pw (g/cc)	2886.67	525.22	516.72	508.15	941.50	
10	2052.5	2525.2	0.38	2000	49	49.2	1	2807.18	531.15	522.75	514.28	906.44	
11	2053.0	2531.1	0.37	2000	50	50.2	VmP (m/s)	2844.53	541.27	532.97	524.60	868.23	
12	2053.5	2541.3	0.36	2000	52	51.5	6038	2881.11	552.73	544.13	535.45	944.53	
13	2054.0	2552.7	0.39	2000	51	50.6	VmS (m/s)	2768.71	516.22	109.18	102.08	965.49	
14	2090.5	2116.2	0.26	2000	16	15.6	4121	3357.58	97.35	88.28	79.12	1549.89	
15	2091.0	2097.4	0.44	2000	10	10.3	pm (g/cc)	2589.12	63.63	55.11	46.51	1410.61	
16	2091.5	2063.6	0.38	2000	7	7.3	2.65	2797.64	38.57	30.48	22.32	1312.25	
17	2092.0	2038.6	0.34	2000	5	4.7	VhP (m/s)	2959.57	798.14	790.34	782.48	472.66	
18	2150.0	2798.1	0.32	2000	73	73.4	3697	3071.07	834.41	826.24	817.99	538.43	
19	2150.5	2834.4	0.35	2000	72	72.3	VhS (m/s)	2929.81	856.14	847.52	838.81	650.05	
20	2151.0	2856.1	0.39	2000	70	69.8	1915	2757.58	873.11	864.49	855.80	630.48	
21	2151.5	2873.1	0.39	2000	71	70.8	ph (g/cc)	2760.82	878.43	869.92	861.33	593.74	
21	2152.0	2878.4	0.38	2000	72	72.0	0.9	2800.26					

Fig.1 A Microsoft Excel based data example to estimate gas hydrate saturation from P-wave velocity only using methods 1 and 2 discussed in text. Columns E and F are estimated hydrate saturations. See text for detail.

Table 1. Parameters used in gas hydrate saturation estimation [data are derived from Helgerud et al (1999) and Lee et al (1996)]. Mineral properties in the KG basin are estimated assuming 90% clay and 10% quartz mineral constituents.

Mineral/fluid	K(GPa)	G(GPa)	ρ (g/cc)	V_p (m/s)	V_s (m/s)	Poisson's ratio
Quartz	36.6	45	2.65	6038	4121	0.06
Clay	20.9	6.85	2.58	3412	1629	0.35
Pure hydrate	7.9	3.3	0.9	3697	1915	0.32
Water	2.25	0	1	1500	0	0.50
Gas	0.11	0	0.23	692	0	0.50
KG basin* (90%clay +10%quartz)	22.15	9.07	2.59	3639	1873	0.32

(Chand et al., 2004), which can be broadly grouped into two categories: 1) empirical relations (Lee et al., 1996) and 2) rock physics based effective medium theory (Helgerud et al., 1999). While the presence of hydrates in the pore space always increases the P-wave velocity of the host sediments, the effect on S-wave velocity depends on the nature and concentration of hydrates within the sediment. Commonly used empirical relationships between V_p and saturations (called four-phase relations involving water, gas, gas hydrate and rock matrix) are:

$$\frac{1}{V_p} = \frac{\phi S_w}{V_w} + \frac{\phi S_g}{V_g} + \frac{\phi S_h}{V_{hP}} + \frac{1-\phi}{V_{mP}} \quad (2)$$

and

$$\frac{1}{\rho V_p^2} = \frac{\phi S_w}{\rho_w V_w^2} + \frac{\phi S_g}{\rho_g V_g^2} + \frac{\phi S_h}{\rho_h V_{hP}^2} + \frac{1-\phi}{\rho_m V_{mP}^2} \quad (3)$$

where V_p , V_w , V_g , V_{hP} , and V_{mP} are the P-wave velocities in the hydrated sediments, water, free-gas, pure hydrate, and matrix, respectively, ϕ is total porosity (as a fraction of rock volume), S_w , S_g , and S_h are the saturations of water, gas, and gas hydrate in the pore space, respectively ($S_w + S_g + S_h = 1$), and ρ_w , ρ_g , ρ_h , ρ_m , and ρ are the densities of water, free gas, pure hydrate, matrix, and bulk sediment, respectively (Table 1). The bulk density ($\rho = \phi S_w \rho_w + \phi S_g \rho_g + \phi S_h \rho_h + (1-\phi)\rho_m$) can be estimated from individual density components. Note that equations 2 and 3 are known as Wyllie's time-average relation and Wood's relation, respectively. The Wood equation is better suited if hydrates are suspended in the pore space, and Wyllie's time average equation is more appropriate if hydrates cement grain contacts. Lee et al (1996) present a weighted mean of the Wood's and time-average equation as

$$\frac{1}{V_p} = \frac{w\phi(1-S_h)^m}{V_{p1}} + \frac{1-w\phi(1-S_h)^m}{V_{p2}} \quad (4)$$

where V_{p1} is P-wave velocity estimated from Wood's equation, V_{p2} is P-wave velocity estimated from time-average equation, w is a weighting factor, and m is a constant simulating the rate of lithification with gas hydrate concentration. The value

of w should be derived from regression analysis of V_p and porosity in hydrate-free sediments and the value of m should be derived from regression analysis of V_p and gas hydrate saturation. Lee et al (1996) used the value of w as 1.1 and the value of m as 1.0. Kumar et al (2007) modified the Wood equation with an effective medium based rock physics relationship that is appropriate for the Hydrate Ridge (offshore Oregon, USA). This effective medium theory assumes that gas hydrate formation reduces the original porosity and becomes part of the solid matrix. The V_p from Modified Wood equation is

$$\frac{1}{\rho V_p^2} = \frac{\phi_m S_w}{\rho_w V_w^2} + \frac{\phi_m S_g}{\rho_g V_g^2} + \frac{1-\phi_m}{\rho_m V_{mP}^2} \quad (5)$$

where $\phi_m = \phi - S_{hyd}$ is porosity after gas hydrate formation, S_{hyd} is the volumetric concentration of gas hydrates in the rock that is now part of the solid matrix, and now gas and water constitute the fluid part in pores ($S_w + S_g = 1$).

The S-wave velocity can be empirically derived. Following hydrate formation model of Kumar et al (2007), V_s can be derived from V_p as follows

$$V_s = V_p \left((1-\phi_m) \frac{V_{mS}}{V_{mP}} \right) \quad (6)$$

where $\frac{V_{mS}}{V_{mP}}$ is the ratio of S to P-wave velocity in the solid matrix and is equal to $\sqrt{G_m / (K_m + 4/3G_m)}$; G_m and K_m are shear modulus and bulk modulus of solid mineral (hydrate and sand/shale minerals). If the gas hydrate formation model is pore filling (not affecting rock framework), then V_s can be estimated according to Lee et al (1996) as

$$V_s = V_p \left[\left((1-\phi) \frac{V_{mS}}{V_{mP}} \right) + \phi S_h \frac{V_{hS}}{V_{hP}} \right] \quad (7)$$

Where $\frac{V_{hs}}{V_{hp}}$ is the ratio of S to P-wave velocity in the pure gas hydrate (which is about 0.46), and solid matrix includes only sand/shale minerals.

Seismic anisotropy and attenuation are also affected by the presence of hydrates/free gas within the sediments, but the relationship of these properties with hydrate saturation is poorly known. Hydrate occurring as vein filling in the sediment can induce seismic anisotropy which can be used to find out the distribution and fabric of gas hydrates (Kumar et al., 2006), but the hydrate concentration estimation using increase in anisotropy due to the presence of gas hydrate is not established. Seismic attenuation in hydrate bearing sediments (especially at sonic frequency) is generally higher than that for the hydrate free sediments (Guerin and Goldberg, 2002). On the other hand, according to Wood et al (2000), gas hydrate formation at the sediment grain contacts rather than in the pore spaces may significantly decrease the seismic attenuation. Wood et al (2000) assumed P-wave seismic attenuation for hydrate-free sediment to be 400 and estimated P-wave seismic attenuation for hydrate-bearing sediment is in the range of 200 to 700. There is a large overlap between the attenuation values for hydrate-free and hydrate-bearing sediments and therefore significant uncertainties exist in gas hydrate saturation estimation using attenuation.

Electrical resistivity

Gas hydrate, like ice, acts as an electrical insulator. The presence of gas hydrate (or free gas) increases the resistivity of rock. For example, downhole resistivity measurements in the northern Cascadia margin have shown a value of ~ 2.0 ohm-m for hydrate bearing sediments in contrast to a value of ~ 1.0 ohm-m for the surrounding sediments (Riedel et al., 2006). Assuming that high resistivity above the BSR is caused by the presence of gas hydrate in pores (meaning pores are filled with water and/or gas hydrate), hydrate saturation can be estimated by Archie's law as proposed by Lu and McMechan (2002)

$$S_h = 1 - S_w = 1 - \left(\frac{R_o}{R_t} \right)^{1/n} \quad (8)$$

where R_o is the resistivity of water saturated formation (background), R_t is the measured resistivity, and n is the exponent. The exponent is about 1.94 for hydrate bearing clastic sediments and is about 1.62 in gas-bearing zone. For example, if resistivity of hydrate-free sediment and hydrate-bearing sediment are 1 ohm-m and 2 ohm-m, respectively, the gas hydrate saturation is about 0.30 according to equation 8. The exponent is empirical and can introduce error in hydrate concentration estimates. The critical factor for hydrate concentration estimation using resistivity data is choosing the baseline indicating hydrate free sediments, which is

dependent on the pore water salinity. Sava and Hardage (2007) suggest calibrating Archie's equation using the Hashim-Shtrikman lower bound on electrical resistivity, and modifying Archie's equation for the presence of clay in hydrate-bearing sediments. Resistivity can be directly measured from well log and estimated from electromagnetic survey. Controlled Source Electromagnetic (CSEM) survey has been recently used for mapping gas hydrate in marine environment (Weitemeyer et al., 2005).

Chloride measurements

Hydrate formation removes water and gas molecules from the pore space and increases the salinity of the surrounding pore water. Conversely, hydrate dissociation during drilling and core recovery releases fresh water, causing pore water to become fresher. Also, in an open system, the excluded ions diffuse away over time after formation of gas hydrates (Yuan et al, 1996; Tinivella, 1999). Ion exclusion of dissolved salts produces distinctive geochemical signatures that are used to identify the presence of gas hydrate and to estimate the hydrate concentration. The main challenge for this method is to accurately predict the base line (background) chlorinity profile. Hyndman et al. (1999) showed that it is possible to estimate both the *in situ* pore fluid salinity and the *in situ* gas hydrate concentration using resistivity data. The chloride anomaly can be used to estimate gas hydrate saturation in the pore space before recovery (Yuan et al., 1996) as

$$S_h = \frac{1}{\rho_h} \left(1 - \frac{Cl_{pw}}{Cl_{sw}} \right) \quad (9)$$

where Cl_{pw} and Cl_{sw} are measured chloride concentrations of pore water and normal bottom seawater (background), respectively. There are various uncertainties in this method as described by Yuan et al (1996). Chloride measurement is performed on core samples extracted during drilling (Tinivella and Carcione, 2001), but the core recovery without damaging it, maintaining *in situ* conditions in laboratory, and finding the right background chloride concentration are some of the difficulties with hydrate concentration estimation with chloride measurements.

NMR-DENSITY porosity

Nuclear magnetic resonance (NMR) logging tool has the ability to measure water-filled porosity, and density porosity measures space occupied by both water and/or gas hydrate (Lee, 2008). In a water-filled formation both NMR- and density-porosities will agree. However, in the hydrate-bearing formations, NMR- and density-porosities will disagree and the difference between the two porosities can be used to estimate gas hydrate saturation as (Lee, 2008),

$$S_h = 1 - \frac{NMR_porosity}{DENSITY_porosity} \quad (10)$$

where NMR_porosity and DENSITY_porosity represent porosities derived from NMR and density log, respectively. Gas hydrate saturation estimation from this method is only possible at well locations.

Density

The formation of gas hydrate reduces the density of rock and this property can be used to estimate hydrate content. Assuming original pore space filled with water and now part of the pore space is filled with gas hydrate, the saturation of gas hydrate can be estimated by knowing the background rock density (ρ_0) for water-filled pores and measured density of hydrate-bearing rock (ρ) as

$$S_h = \frac{1}{\phi} \frac{\rho_0 - \rho}{\rho_w - \rho_h} \quad (11)$$

The density measurement and therefore hydrate saturation estimation is possible from well logs derived density and three dimensional density derived from seismic data AVA inversion.

Temperature

Gas hydrate dissociation is an endothermic process. Once gas hydrate dissociates, sediment containing hydrate is cooled relative to the surrounding sediment, thus creating a negative temperature anomaly (Ford et al., 2003). During recent deep-sea drillings, infrared thermal imaging camera has been used to image sediment cores and negative temperature anomaly (average 4°C cooler) has been identified due to gas hydrate. Thermal method at drilling locations has often been used for qualitative identification of gas hydrates.

Among the six methods discussed above, some are remote sensing methods (seismic, electrical), and others involve direct measurements from downhole logging (seismic, electrical, NMR-DENSITY porosity, density) and coring (chloride, temperature). Each method (or data type) has its own accuracy, sensitivity and cost issue. Seismic methods are the most common but the estimated gas hydrate concentration can be less accurate than coring method. Although coring method has certain difficulty such as the core sampling, preserving samples in *in situ* condition, and making laboratory measurements on core samples, but it provides more accurate prediction of hydrate concentration. Evidently, remote sensing and logging methods are *in situ* measurements and coring methods require laboratory measurements.

Implementation of the Seismic Methods

Seismic velocity is most commonly used to derive

gas hydrate saturation. Gas hydrate saturation estimation from seismic velocity is an inverse problem where one tries to find the hydrate saturation for which modeled velocity best matches with measured velocity. Actual calculations are typically done with software/scripts written in a high-level computer language like Java, C, Fortran, Matlab, or Microsoft Excel. Here, we discuss two simple implementation methods of estimating gas hydrate saturation from seismic velocity: using a look-up table or regression analysis (method 1) and a direct estimation method (method 2). The difference between the two methods is in implementation, and the method 1 is more general. The gas saturation is ignored for simplification, but in the case of free gas and gas hydrate coexisting both can be simultaneously estimated. The steps for hydrate saturation estimation in method 1 are: 1) first create a table of modeled seismic velocity (V_p and/or V_s) using a preferred velocity modeling method for various gas hydrate saturations and given porosity values, 2) compute velocity mismatch (difference of modeled and measured velocities), and 3) look up for the minimum velocity mismatch created in step 2; the corresponding gas hydrate saturation (S_h) represents an estimate of gas hydrate. This can be done with V_p only and more reliably with both V_p and V_s simultaneously. The hydrate saturation estimation using method 2 can be simply performed by rewriting the velocity modeling equation for S_h . The method 2 can be used with only one velocity (V_p), modeled with either the time-average equation for V_p (equation 2) or the Wood relation for V_p (equation 3). The equations for estimating hydrate saturation (method 2) using the time-average equation and the Wood equation are

$$S_h = \left[\frac{1}{\phi} \left(\frac{1}{V_P} - \frac{1}{V_{mP}} \right) - \left(\frac{1}{V_w} - \frac{1}{V_{mP}} \right) \right] / \left(\frac{1}{V_{hP}} - \frac{1}{V_w} \right) \quad (12)$$

and

$$S_h = \left[\frac{1}{\phi} \left(\frac{1}{\rho V_P^2} - \frac{1}{\rho_m V_{mP}^2} \right) - \left(\frac{1}{\rho_w V_w^2} - \frac{1}{\rho_m V_{mP}^2} \right) \right] / \left(\frac{1}{\rho_h V_{hP}^2} - \frac{1}{\rho_w V_w^2} \right) \quad (13)$$

where V_p is the measured P-wave velocity and S_h is the gas hydrate saturation. In both methods 1 and 2, the common requirements are: the matrix properties, the velocity for hydrate-free sediments (background velocity), and calibration of modeled and measured velocities. The calibration of modeled and measured velocities is to make sure that for the background case (hydrate-free sediments) modeled and measured velocities are in agreement. In this paper, in method 1 the modeled velocity is calibrated (say by multiplying with scalar1) before computing velocity error and in method 2 the measured velocity is calibrated (say by multiplying with scalar2). Assuming that the background measured P-wave velocity is V_{Pback} , and the modeled P-wave velocity (for $S_h = 0$) is V_{Psh0} , the scalar1 ($=V_{Pback}/V_{Psh0}$) is the ratio of V_{Pback} and V_{Psh0} and the scalar2 ($=V_{Psh0}/V_{Pback}$) is the ratio of V_{Psh0} and V_{Pback} .

The methods 1 and 2 can be simply performed in a Microsoft Excel sheet. Figure 1 shows a data example to compute gas hydrate saturation from V_p alone with both methods 1 and 2. The V_p in this example is modeled with Wyllie's time average equation (equation 2) for hydrate bearing sediments in the absence of free gas, and assuming clean sand (quartz as mineral). Data in columns A to C are from a well log, column D is background V_p for hydrate-free sediments, column G is various input parameters (Table 1), column H is background modeled V_p (V_{psh0}) using the Time-average equation, and columns J to DF is a table of absolute velocity difference (modeled calibrated V_p – measured V_p) for various gas hydrate saturations and porosities. The columns M through DE in Figure 1 are hidden. The actual script used to calculate J5 in the table (Figure 1) is $ABS((1/(C5*J\$3/\$G\$7+C5*J\$2/\$G\$3+C5*J\$4/\$G\$17+(1-C5)/\$G\$11))*D5/H5-B5)$, where D5/H5 is scalar1. The column E is gas hydrate saturation estimated from method 1, and the actual script used to calculate E5 is $INDEX(J\$4:DF\$4,1,MATCH(MIN(J5:DF5),J5:DF5,0))*100$. The column F is gas hydrate saturation estimated from method 2, and the actual script to calculate F5 is $(1/C5*(1/(B5*H5/D5)-1/\$G\$11)-(1/\$G\$7-1/\$G\$11))/(1/\$G\$17-1/\$G\$7)*100$. The gas hydrate saturation is calculated for each depth point (one data point in one row, Figure 1). Note that saturations estimated from methods 1 and 2 are same, and to estimate gas hydrate saturation using method 2 only column H (modeled V_p for $S_h=0$) is needed and not the velocity error table, however, method 2 can only be used with V_p , and when V_p is either modeled with an equation (the time-average equation or the Wood's equation in this article) that can be rewritten for the forward computation of hydrate saturation in terms of V_p , density and porosity (as given in equations 12 and 13).

We recommend using both V_p and V_s simultaneously if available, and in this case one will have to use method 1 to estimate gas hydrate. The Figure 1 is an example of Microsoft Excel scripts to calculate gas hydrate saturation. The estimated hydrate saturation will be different due to differences in 1) velocity modeling methods, 2) background models and 3) mineral/fluid properties.

Field Data Examples

We discuss data examples from three fields: Alaska, Cascadia margin, and Krishna Godawari (KG) basin. With the Alaska data, we show a typical well log data in hydrate bearing sediments, and compare estimated hydrate saturation from various data/methods assuming quartz as the mineral matrix. With the Cascadia margin data example, we compare hydrate saturation estimated from different data/methods (again assuming quartz as the mineral matrix) and discuss the effect of varying background model on hydrate saturation. With the KG basin data, we compare estimated hydrate saturation from various data/methods, and discuss the effect of varying mineral properties on hydrate saturation. The rock matrix is quartz (sand) rich in the first two data examples, but is clay rich (90% clay and 10% quartz) in the case of KG basin.

Mount Elbert test data, Alaska

BP-DOE-USA consortium conducted a well test in 2007 called "Mount Elbert test" to study the feasibility of hydrate exploration and exploitation in Alaska (Inks and Agena, 2008; Boswell et al., 2008). The well-log data can be requested free of cost from NETL (National Energy Technology Laboratory)

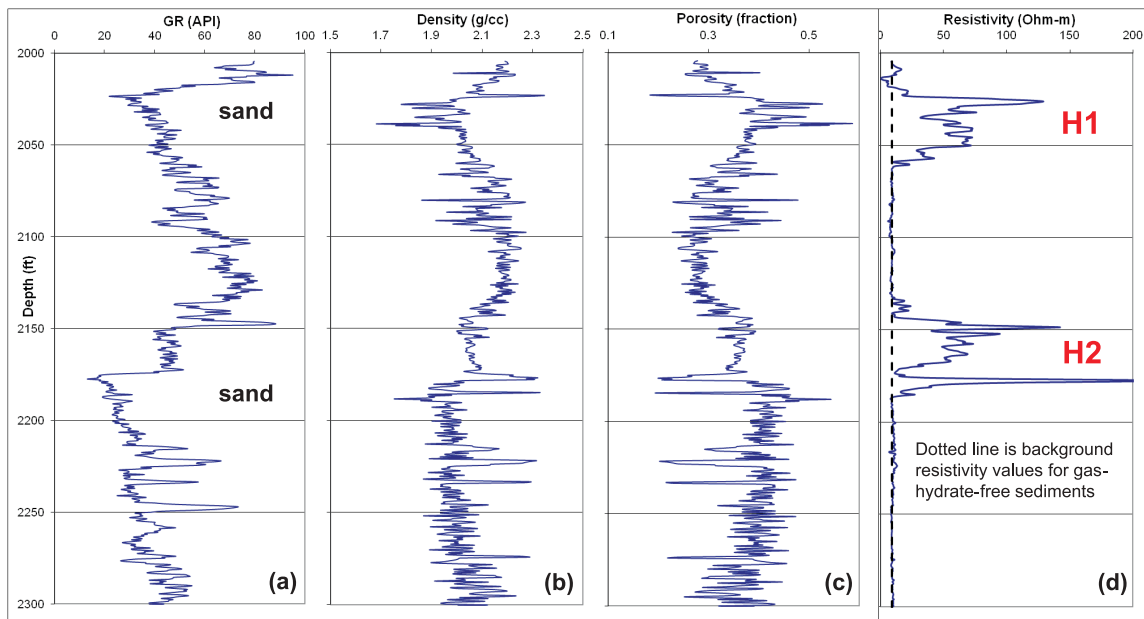


Fig.2 Well logs from Mount Elbert #1: a) gamma ray log, b) density log, c) porosity log, and d) deep resistivity log. Two possible gas hydrate zones are marked as H1 and H2. These two zones H1 and H2 are Units D and C in Inks and Agena (2008), respectively. It is evident that hydrate layers are identified in higher porosity sands because of higher seismic velocities (shown in Figure 3), lower density and higher resistivity than hydrate-free background layers.

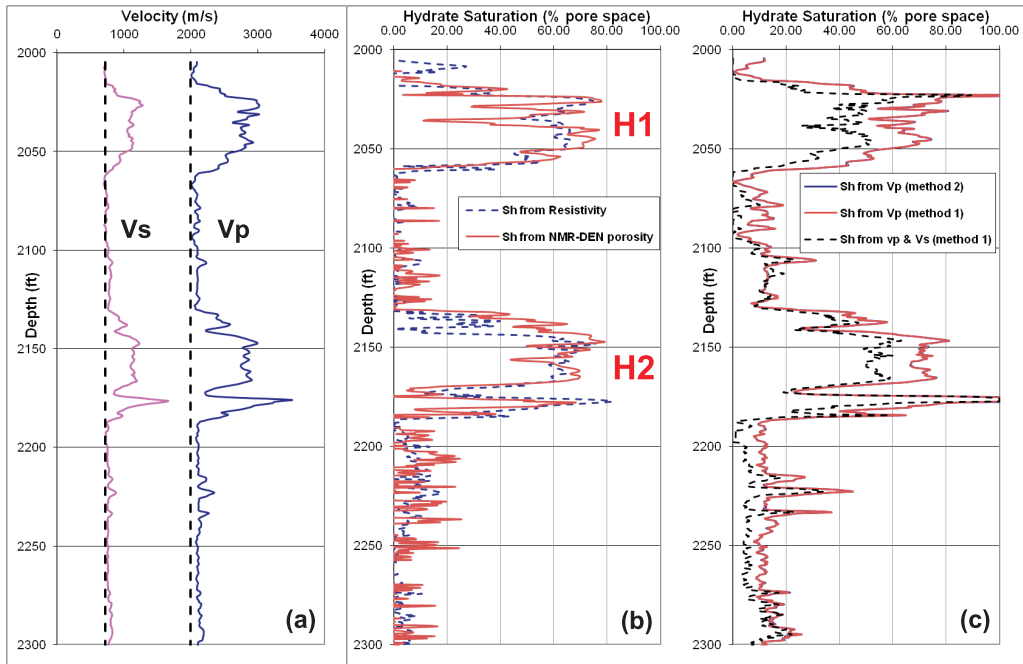


Fig.3 Gas hydrate saturation estimated from well logs at Mount Elbert #1. On the left are V_p and V_s logs with corresponding background values plotted by black dotted vertical lines (a), and in the middle panel (b) is gas hydrate saturation derived from resistivity log (blue dotted line) using equation 8 and from NMR-DENSITY porosity logs (red solid line) using equation 10. The right panel (c) shows gas hydrate saturations estimated from seismic velocities: blue and red color solid curves show saturations estimated from V_p alone using method 2 and method 1, respectively (they are indistinguishable), and black dotted curve show hydrate saturation estimated from both V_p and V_s simultaneously. In this example, V_p is modeled using equation 2 and V_s is modeled using equation 7.

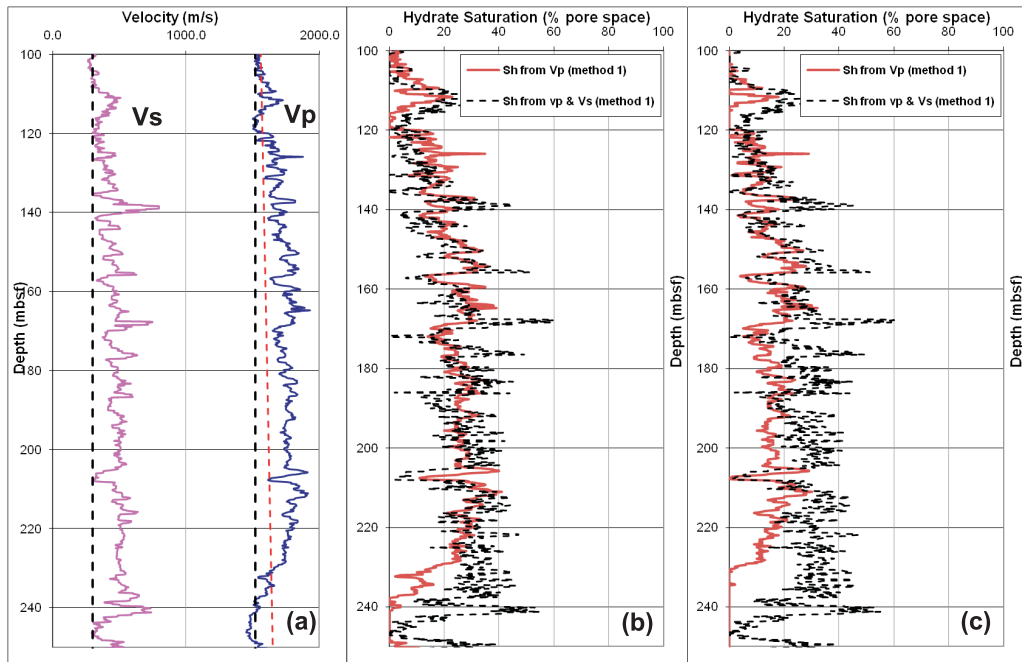


Fig. 4 Gas hydrate saturation estimated from well logs at northern Cascadia margin, Expedition 311 site U1327E. On the left (a) are V_p and V_s logs with corresponding background values plotted by black dotted vertical lines and another background depth varying V_p (red dotted line) from Yuan et al (1996). The middle panel (b) and the right panel (c) show gas hydrate saturations estimated from V_p alone (red solid curve) and V_p and V_s combined (black dotted curve) using method 1. The estimated hydrate saturation shown in the middle panel uses constant background velocities (black vertical dotted lines in Figure 4a), and saturation shown in the right panel were estimated using a constant background value for V_s as in the middle panel and a depth varying V_p trend (red dotted curve in Figure 4a). Note the change in hydrate saturation (middle vs. right panels) due to change in background V_p value only. In this example, V_p is modeled using equation 2 and V_s is modeled using equation 7. Depth shown is in mbsf (meters below seafloor), water depth is 1300m and the BSR is at 225mbsf.

website (<http://www.netl.doe.gov/technologies/oil-gas/FutureSupply/MethaneHydrates/ANSLogData.html>). An example of the well logs from the Mount Elbert site is shown in Figures 2 and 3, where Depth is measured from KB (54.80ft above sea level). Gas hydrate saturation can be estimated from resistivity log using equation 8 knowing the background resistivity of hydrate-free sediments. In this example, we assume a background resistivity of 9 ohm-m. Given the NMR-porosity and density porosity logs, gas hydrate saturation (Figure 3) is estimated using equation 10. For hydrate saturation estimation using seismic velocities, we assume a constant background value of V_p (2000 m/s) and V_s (720 m/s) as shown by black dotted lines in Figure 3. Figure 3c shows gas hydrate saturations estimated from V_p alone (using both methods 1 and 2 as described earlier) and from both V_p and V_s together. In this example, hydrate saturation varies from 40% to 80% of pore space in the GHSZ.

Cascadia margin, IODP Expedition 311 data, Canada

The northern Cascadia continental margin offshore western Canada is under study for the last two decades and the presence of gas hydrates is confirmed from many geophysical and geological experiments. More recently, an extensive list of log data were acquired at five locations (U1325 to U1329) through IODP Expedition 311 in 2005 to study the geological models for the formation of hydrates as well as to estimate hydrate concentration (Riedel et al., 2006). The drillhole locations were chosen so as to study the formation (and dissociation) of gas hydrates within the accretionary prism at different stages of its development away from the Juan de Fuca ridge. Chen (2006) did an elaborative study of the different logs from IODP Expedition 311 to estimate the hydrate concentration. Combined seismic reflection and sonic log study by Dash (2007) showed a hydrate saturation of about ~15% of pore space at IODP Site U1327, where the BSR depth is 225 mbsf (meters below seafloor). Figure 4 shows hydrate saturation estimated from seismic velocities with a constant background V_s trend and two different background V_p trends. The estimated hydrate saturations vary by changing the background V_p trend, which emphasizes the importance of a reliable background model. In this example, hydrate saturation varies from 10% to 40% of pore space in the GHSZ.

KG basin, NGHP Expedition -1 data, India

The Government of India started the National Gas Hydrate Program (NGHP) in 1997 to explore gas hydrate resources in India. The presence of gas-hydrate in the Indian continental margin was confirmed during drilling/coring onboard JOIDES Resolution between 28th April 2006 and 19th August 2006 (Collett et al., 2008). This is known as NGHP Expedition 01. The drilling/coring revealed 128 m thick gas hydrate in the KG offshore basin predominantly deposited in the fracture network (Holland et al., 2008), disseminated deposits of varying thickness in the Mahanadi basin and

Andaman basin. We illustrate the methods of hydrate saturation estimation from the well logs acquired in KG offshore basin during NGHP Expedition 1 (Collett et al., 2008). The sedimentological parameters measured onboard suggest that the matrix minerals are composed of 90 % clay and 10 % quartz. We use Hill's averaging method (Hill, 1952) to estimate matrix effective elastic moduli from the pure mineral phases. According to Hill's averaging, the bulk modulus and the shear modulus of clay and quartz mix mineral are

$$K_m = \frac{1}{2} \left([V_{clay} K_{clay} + V_{qtz} K_{qtz}] + \left[\frac{V_{clay}}{K_{clay}} + \frac{V_{qtz}}{K_{qtz}} \right]^{-1} \right) \quad (14)$$

and

$$G_m = \frac{1}{2} \left([V_{clay} G_{clay} + V_{qtz} G_{qtz}] + \left[\frac{V_{clay}}{G_{clay}} + \frac{V_{qtz}}{G_{qtz}} \right]^{-1} \right) \quad (15)$$

where V_{clay} and V_{qtz} stand for clay and quartz volume fraction of mineral, K_{clay} and K_{qtz} are the bulk moduli of clay and quartz, G_{clay} and G_{qtz} are the shear moduli of clay and quartz, respectively. The mineral density can be estimated by volume averaging as $\rho_m = V_{clay} \rho_{clay} + V_{qtz} \rho_{qtz}$, where ρ_{clay} and ρ_{qtz} are density of clay and quartz minerals (Table 1). Knowing elastic moduli and density, P- and S-wave velocities in mineral can be estimated as $V_{mP} = \sqrt{(K_m + 4/3 G_m) / \rho_m}$ and $V_{mS} = \sqrt{G_m / \rho_m}$, respectively. Figure 5 shows gas hydrate saturation estimated at this well location from resistivity (Figure 5a) and seismic velocities (sonic logs) data (Figures 5b and 5c). For hydrate saturation estimation from seismic velocity using method 1, linear background velocities for P- and S-waves were assumed, and seismic velocities were modeled assuming 90% clay and 10% quartz as mineral in Figure 5b and 100% quartz as mineral in Figure 5c. Hydrate saturation is different if 100% quartz is assumed as mineral composition compared to 90% clay and 10% quartz as mineral composition. The base of hydrate stability zone is clearly demarcated in the hydrate saturation plots at about 185 mbsf. This data example emphasizes the importance of knowing the correct mineral composition. Hydrate saturation varies from 5% to 40% of pore space in the GHSZ.

Discussions and Conclusions

There are various direct and indirect methods for estimating gas hydrate concentration. The reliability of the gas hydrate concentration will depend on 1) the quality of measured data, 2) reliability of the relationship between the rock's physical property (e.g., seismic velocity, resistivity) and gas hydrate concentration, 3) background property values in the absence of gas hydrates, and 4) *in situ* conditions. If there is any discrepancy among hydrate concentration estimated from different data and methods, one should look at all the four issues. Lee and Collett (2006) discuss errors in gas hydrate saturation estimation due to

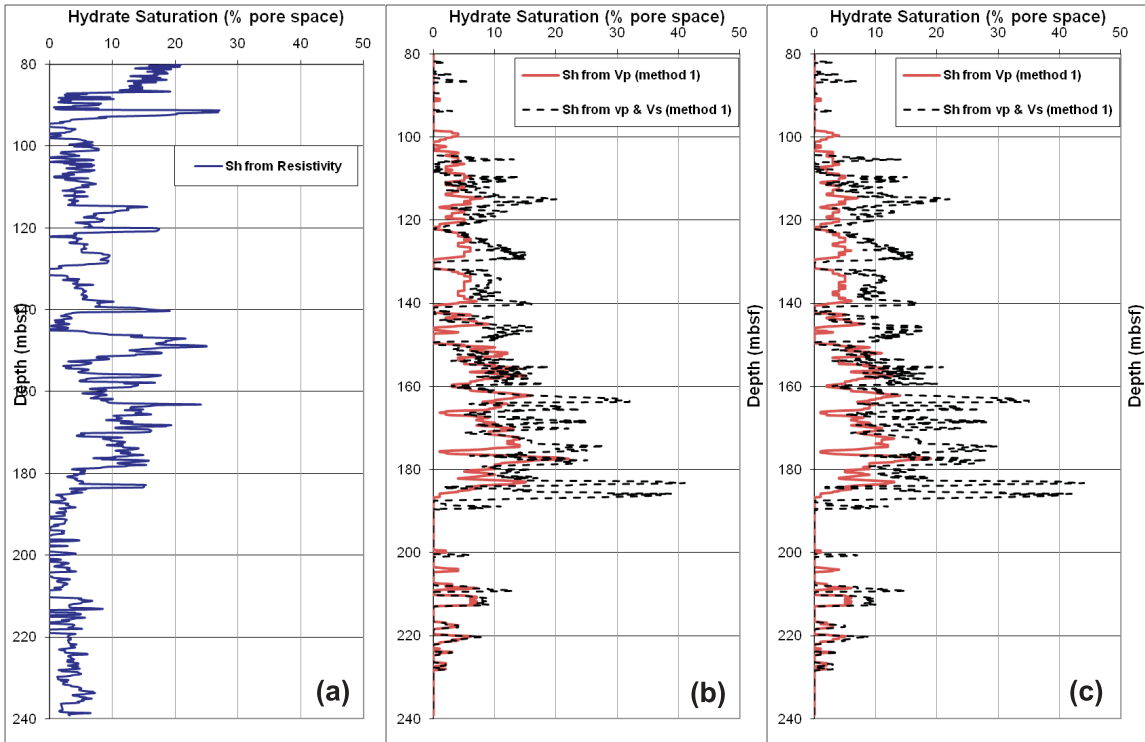


Fig. 5 Gas hydrate saturation estimated from well logs in KG basin. On the left (a) is hydrate saturation estimated using resistivity log with 1.08 ohm-m as the background resistivity value. The middle panel (b) and the right panel (c) show gas hydrate saturations estimated from V_p alone (red solid curve) and V_p and V_s combined (black dotted curve) using method 1, with linear background velocities [V_p (m/s)=depth(mbsf)*0.6+1546.67, and V_s (m/s)=depth(mbsf)*0.492+210.67]. Seismic velocities were modeled assuming 90% clay and 10% quartz as mineral composition in Figure 5b and 100% quartz as mineral composition in Figure 5c. Note the differences in hydrate saturation due to differences in mineral compositions (Figures 5b and 5c). In this example, V_p is modeled using equation 2 and V_s is modeled using equation 7. A linear increase in the hydrate concentration is observed from 100 mbsf to 185 mbsf. The base of the hydrate stability zone is clearly demarcated in the hydrate saturation plot at about 185 mbsf.

uncertainties in measurement and properties. If the measured data are reliable, one should carefully decide about an empirical equation or rock physics based equation to model physical properties of the gas hydrate-bearing sediments. In this paper we used only Wyllie's equation to model V_p and empirical equation 7 to model V_s . The two most important factors in estimating a reliable hydrate concentration are: 1) knowledge of background property trend, and 2) physical property modeling method. In this paper we discussed various methods of hydrate concentration estimation using three data sets. For hydrate saturation estimation from seismic velocity, we discussed the importance of background model, *in situ* mineral composition, and velocity modeling method. We also presented a workflow to estimate hydrate saturation from seismic velocity in a Microsoft Excel sheet.

Acknowledgements

We thank Chevron and Director, National Institute of Oceanography Goa for permission to publish this paper. We also thank Mrinal K Sen for reviewing manuscript. Mount Elbert data from Alaska are courtesy of US Department of Energy and BP Exploration, Alaska, Inc., Northern Cascadia data are from IODP, and KG basin data were acquired onboard JOIDES Resolution during NGHP Expedition 1 under the aegis of Directorate General of

Hydrocarbons (DGH). This is N10 contribution no. 4652.

References

- Boswell, R., Hunter, R., Collett, T., Digert, S., Hancock, S., Weeks, M., and Mount Elbert Science Team, 2008, Investigation of gas hydrate-bearing sandstone reservoirs at the "Mount Elbert" Stratigraphic test well, Milne Point, Alaska: Proceedings of the 6th International Conference on Gas Hydrates, Vancouver, BC, Canada, July 6-10
- Carcione, J. M., and Gei, D., 2004, gas-hydrate concentration estimated from P- and S-wave velocities at the mallik 2L-38 research well, Mackenzie Delta, Canada: J. Applied Geophysics, 56, 73-78.
- Chand, S., Minshull, T. A., Davide, G., and Carcione, J. M., 2004, Elastic velocity models for gas-hydrate-bearing sediments-a comparison: Geophys. J. Int., 159 (2), 573-590.
- Chen M., 2006, Northern Cascadia marine gas hydrate: constraints from resistivity, velocity, and AVO: MSc thesis, University of Victoria; 165 pp.
- Collett, T. S., 2002, Energy resource potential of natural gas hydrates: AAPG Bulletin, 86, 1971-1992.
- Collett, T. S., Reidel, M., Cochran, J. R., Boswell, R., Presley, J.,

- Kumar, P., Sathe, A., Sethi, A., Lall, M., and Sibal, V., 2008, Indian National Gas Hydrate Program: Expedition 01-initial report, Vol. 1, Directorate General of Hydrocarbon, New Delhi, India.
- Dai, J., Xu, H., Synder, F., and Dutta, N., 2004, Detection and estimation of gas hydrates using rock physics and seismic inversion: examples from the northern deepwater Gulf of Mexico: *The Leading Edge*, 23, 60-66.
- Dash R., 2007, Crustal structure and marine gas hydrate studies near Vancouver Island using seismic tomography: PhD thesis, University of Victoria, 152 pp.
- Ecker, C., Dvorkin, J., and Nur, A., 2000, Estimating the amount of gas hydrate and free gas from marine seismic data: *Geophysics*, 65, 565-573.
- Ford, K. H., Naehr, T. H., Skilbeck, C. G., and the Leg 201 Scientific Party, 2003, The use of infrared thermal imaging to identify gas hydrate in sediment cores. *In* D'Hondt, S. L. Jorgensen, B. B., Miller, D. J., et al. (Eds.), *Proc. ODP, Init. Rets.*, 201, 1-20. Online at http://www-odp.tamu.edu/publications/201_IR/VOLUME/CHAPTERS/IR201_04.PDF.
- Guerin, G., Goldberg, D., 2002, Sonic waveform attenuation in gas hydrate-bearing sediments from the JAPEX/JNOC/GSC Mallik 2L-38 research well, Mackenzie Delta: Canada, *J. Geophys. Res.* 107(B5), 2088, doi:10.1029/2001JB000556.
- Helgerud, M. B., Dvorkin, J., Nur, A., Sakai, A., and Collett, T., 1999, Effective wave velocity in marine sediments with gas hydrates: Effective medium modeling: *Geophys. Res. Lett.*, 26, 2021-2024.
- Hill, R., 1952, The elastic behavior of crystalline aggregate: *Proc. Phys. Soc., London*, A65, 349-354.
- Holland, M., Schultheiss, P., Roberts, J., and Druce, M., 2008, Observed gas hydrate morphologies in marine sediments: Proceedings of the 6th International Conference on Gas Hydrates, Vancouver, BC, Canada, July 6-10.
- Hyndman, R.D., Yuan, T., and Moran, K., 1999. The concentration of deep sea gas hydrates from downhole electrical resistivity logs and laboratory data: *Earth Planet. Sci. Lett.*, 172:167-177. doi:10.1016/S0012-821X(99)00192-2.
- Inks, T. L., and Agena, W. F., 2008, Successful gas hydrate prospecting using 3D seismic-a case study for the Mt. Elbert prospect, Milne Point, North Slope Alaska: SEG expanded abstract, 473-477.
- Kumar, D., Sen, M. K., Bangs, N. L., Wang, C., and Pecher, I., 2006, Seismic anisotropy at Hydrate Ridge: *Geophys. Res. Lett.*, 33, L01306, doi:10.1029/2005GL023945.
- Kumar, D., Sen, M. K., and Bangs, N. L., 2007, Gas hydrate concentration and characteristics within Hydrate Ridge inferred from multicomponent seismic reflection data: *J. Geophys. Res.*, 112, B12306, doi:10.1029/2007JB004993.
- Korenga, J., Holbrook, W. S., Singh, S. C., and Minshull, T. A., 1997, Natural gas hydrates on the southeast US margin: Constraints from full-waveform and travelttime inversion of wide-angle seismic data: *J. Geophys. Res.*, 102, 15345-15365.
- Kvenvolden, K. A., 1999, Potential effects of gas hydrate on human welfare: Proceedings of the National Academy of Science, USA, 96, 3420-3426.
- Lee, M. W., 2008, Models for gas hydrate-bearing sediments inferred from hydraulic permeability and elastic velocities: USGS Scientific Investigations Report 2008-5219, 14p, online at http://pubs.usgs.gov/sir/2008/5219/pdf/SIR08-5219_508.pdf.
- Lee, M. W., and Collett, T. S., 2006, Gas hydrate and free gas saturations estimated from velocity logs on Hydrate Ridge, offshore Oregon, USA. *In* Tréhu, A. M., Bohrmann, G., Torres, M. E., and Colwell, F. S. (Eds.), *Proc. ODP, Sci. Results*, 204, 1-25. Online at: http://www-odp.tamu.edu/publications/204_SR/VOLUME/CHAPTERS/103.PDF.
- Lee, M. W., Hutchinson, D. R., Collett, T. S., and Dillon, W. P., 1996, Seismic velocities for hydrate-bearing sediments using weighted equation: *J. Geophys. Res.*, 101, 20347-20358.
- Lu, S., and McMechan, G. A., 2002, Estimation of gas hydrate and free gas saturation, concentration, and distribution from seismic data: *Geophysics*, 67, 582-593.
- Milkov, A. V., 2004, Global estimates of hydrates-bound gas in marine sediments: how much is really out there?: *Earth-Science Reviews*, 66, 183-197
- Ojha, M., and Sain, K., 2007, Seismic modeling and quantification of gas-hydrates from AVA modeling in the western continental margin of India: *Mar. Geophys Res.*, 28, 101-107.
- Riedel, M., Willoughby, E. C., Chen, M. A., He, T., Novosel, I., Schwalenberg, K., Hyndman, R. D., Spence, G. D., Chapman, N. R., and Edwards, R. N., 2006, Proceedings of the Integrated Ocean Drilling Program, Volume 311.
- Sava, D. C., and Hardage, B. A., 2007, Gas-hydrate concentration and uncertainty estimation from electrical-resistivity logs: Examples from Green Canyon, Gulf of Mexico: SEG expanded abstracts, 26, 1579-1583.
- Singh, S. C., Minshull, T. A., and Spence, G. D., 1993, Velocity structure of a gas hydrate reflector: *Science*, 260, 204-207.
- Sloan, E. D. Jr., 1998, *Clathrate Hydrates of Natural Gases*, Marcel Dekker, New York.
- Tinivella, U., 1999, A method for estimating gas hydrate and free gas concentrations in marine sediments: *Boll. Geof. Teor. Appl.*, 40, 19-30.
- Tinivella, U., and Carcione, J., 2001, Estimation of gas-hydrate concentration and free-gas saturation from log and seismic data: *The Leading Edge*, 20, 200-203.

- Yuan, T., Hyndman, R. D., Spence, G. D., and Desmons, B., 1996, Seismic velocity increase and deep-sea hydrate concentration above a bottom-simulating reflector on the northern Cascadia continental slope: *J. Geophys. Res.*, 101, 13655-13671.
- Yun, T. S., Francisca, F. M., Santamarina, J. C., and Ruppel, C., 2005, Compressional and shear wave velocities in uncemented sediment containing gas hydrate, *Geophys. Res. Lett.*, 32, doi:10.1029/2005GL022607.
- Waite, W., Helgerud, M. B., Nur, A., Pinkston, J. C., Stern, L., and Kirby, S., 2000. Laboratory measurements of compressional and shear wave speeds through methane hydrate: *In Gas Hydrates: Challenges for the Future*, edited by G. D. Holder and P. R. Bishnoi, *Ann. N.Y. Acad. Sci.*, 912, 1003– 1010.
- Weitemeyer, K. A., Constable, S. C., Ket, K. W., and Behrens, J. P., 2005, First result from a marine control-source electromagnetic survey to detect gas hydrates offshore Oregon: *Geophys. Res. Lett.*, 33, L03304, doi:10.1029/2005GL024896.
- Westbrook, et al., 2008, Estimation of gas hydrate concentration from multi-component seismic data at sites on the continental margins of NW Svalbard and the Storegga region or Norway: *Marine and Petroleum Geology*, 25, 744-758.
- Willoughby, E. C., and Edwards, R. N., 1997, On the resource evaluation of marine gas-hydrate deposits using seafloor compliance methods: *Geophys. J. Int.*, **131**, 751-766.
- Wood, W. T., Holbrook, W. S., and Hoskins, H., 2000, In situ measurements of P-wave attenuation in the methane hydrate- and gas-bearing sediments of the Blake Ridge. *In Paul, C. K., Matsumoto, R., Wallace, P. J., and Dillon, W. P. (Eds.), Proc. ODP, Sci. Results*, 164, 265-272.
- Corresponding author: Dhananjay Kumar (dhananjaykumar@gmail.com)*